AMERICAN SOCIETY FOR MICROBIOLOGY | Infection and Immunity®

HOST RESPONSE AND INFLAMMATION

MyD88-Dependent Glucose Restriction and Itaconate Production Control *Brucella* Infection

Carolyn A. Lacey,[a,b] Bárbara Ponzilacqua-Silva,[a,b] Catherine A. Chambers,[a,b] Alexis S. Dadelahi,[a,b] Jerod A. Skyberg[a,b]

[a]Department of Veterinary Pathobiology, College of Veterinary Medicine, University of Missouri, Columbia, Missouri, USA
[b]Laboratory for Infectious Disease Research, University of Missouri, Columbia, Missouri, USA

Carolyn A. Lacey and Bárbara Ponzilacqua-Silva contributed equally to this work. Author order was determined by seniority.

ABSTRACT Brucellosis is one of the most common global zoonoses and is caused by facultative intracellular bacteria of the genus *Brucella*. Numerous studies have found that MyD88 signaling contributes to protection against *Brucella*; however, the underlying mechanism has not been entirely defined. Here, we show that MyD88 signaling in hematopoietic cells contributes both to inflammation and to control of *Brucella melitensis* infection *in vivo*. While the protective role of MyD88 in *Brucella* infection has often been attributed to promotion of gamma interferon (IFN-γ) production, we found that MyD88 signaling restricts host colonization by *B. melitensis* even in the absence of IFN-γ. *In vitro*, we show that MyD88 promotes macrophage glycolysis in response to *B. melitensis*. Interestingly, a *B. melitensis* mutant lacking the glucose transporter, GluP, was more highly attenuated in MyD88$^{-/-}$ than in wild-type mice, suggesting MyD88 deficiency results in an increased availability of glucose *in vivo*, which *Brucella* can exploit via GluP. Metabolite profiling of macrophages identified several metabolites regulated by MyD88 in response to *B. melitensis*, including itaconate. Subsequently, we found that itaconate has antibacterial effects against *Brucella* and also regulates the production of proinflammatory cytokines in *B. melitensis*-infected macrophages. Mice lacking the ability to produce itaconate were also more susceptible to *B. melitensis in vivo*. Collectively, our findings indicate that MyD88-dependent changes in host metabolism contribute to control of *Brucella* infection.

KEYWORDS brucellosis, MyD88, IRG1, itaconic acid

Bacteria of the genus *Brucella* cause brucellosis, one of the most common zoonotic infections in the world, infecting over 500,000 individuals each year (1). *Brucella* species infect a variety of domestic livestock, such as cattle, goats, pigs, and sheep, which provide a reservoir for human infection. Humans are usually infected via consumption of unpasteurized dairy products or through inhalation of infectious aerosols (2, 3). Human brucellosis is a severely debilitating disease that typically requires hospitalization (4). Brucellosis is characterized by persistent waves of fever with systemic symptoms that can vary among individuals, including chills, malaise, headaches, and hepato- or splenomegaly (5). Osteoarticular and/or musculoskeletal inflammation are the most common focal complications of brucellosis, with an incidence of 40 to 80% in infected individuals (6, 7). *Brucella*-induced arthritis can be treated with prolonged antibiotic therapy; however, the time to resolve inflammation can be extensive, and disease can relapse (7, 8).

Myeloid differentiation factor 88 (MyD88) is an adaptor protein that relays Toll-like receptor (TLR), interleukin-1R (IL-1R), and IL-18R signaling (9, 10). *Brucella* reportedly can be recognized by host cells via TLR2, TLR4, TLR6, and TLR9 (11–15). Upon ligand

Citation Lacey CA, Ponzilacqua-Silva B, Chambers CA, Dadelahi AS, Skyberg JA. 2021. MyD88-dependent glucose restriction and itaconate production control *Brucella* infection. Infect Immun 89:e00156-21. https://doi.org/10.1128/IAI.00156-21.

Editor Guy H. Palmer, Washington State University

Address correspondence to Jerod A. Skyberg, skybergj@missouri.edu.

Received 5 April 2021
Returned for modification 26 April 2021
Accepted 5 June 2021
Accepted manuscript posted online 14 June 2021
Published 16 September 2021

binding, TLRs can signal through MyD88, which can result in the production of cytokines (16). IL-12 production by macrophages and dendritic cells in response to *Brucella* is dependent on MyD88 signaling (17). MyD88 also mediates signal transduction in response to IL-18, and IL-12 and IL-18 can synergize to induce production of gamma interferon (IFN-γ) (18). As MyD88 promotes IFN-γ production, which, in turn, is essential for control of *Brucella* infection, the protective effect of MyD88 against *Brucella* has often been attributed to IFN-γ or to the production of other proinflammatory cytokines (17, 19). However, in addition to promoting cytokine production, TLR stimulation and subsequent signaling through MyD88 can also promote glycolysis and glucose consumption by host cells (20, 21). While MyD88 is protective against a number of pathogens, how MyD88 alters host metabolism to restrict bacterial infection has not been well studied. Therefore, in this study we sought to clarify the role of host metabolism and IFN-γ in MyD88-dependent protection against *Brucella* infection.

RESULTS

Hematopoietic MyD88 signaling mediates inflammation and control of *B. melitensis* infection. Previously, we demonstrated that MyD88 signaling contributes to both inflammation and control of *Brucella* infection within the joint following footpad infection (22). *Brucella* can infect a variety of phagocytic and nonphagocytic cells (23). To determine the cells that harbor *B. melitensis* within the joint and potentially contribute to MyD88-dependent immune responses, we sorted live cells from infected joints via flow cytometry. Nonhematopoietic cells (CD45.2$^-$), macrophages (CD45.2$^+$/F4/80$^+$), neutrophils (CD45.2$^+$/Ly-6G$^+$), and other CD45.2$^+$ hematopoietic cells (hematopoietic cells that were not neutrophils or macrophages) were sorted from *B. melitensis*-infected joints via flow cytometry, and these populations were plated onto agar to determine the relative amount of *Brucella* in each cell type. Similar to what we previously reported (22, 24), *B. melitensis* infection caused a robust increase in the proportion of hematopoietic cells, particularly neutrophils and macrophages within the joint, after infection (see Fig. S1A in the supplemental material). One day postinfection, similar numbers of *B. melitensis* were recovered from all cell types on a per-sorted-cell basis (Fig. S1B), and, proportionally, 43% of viable *B. melitensis* was recovered from nonhematopoietic cells, with 25%, 12%, and 19% recovered from macrophages, neutrophils, and other hematopoietic cells, respectively (Fig. S1C). By day 3 postinfection, macrophages on average harbored more *Brucella* per sorted cell than did nonhematopoietic cells, neutrophils, or other hematopoietic cells (Fig. S1B) and contained ~40% of the recovered *B. melitensis* (Fig. S1C).

As *Brucella* was detected in both hematopoietic and nonhematopoietic cells within the joint (Fig. S1), we next investigated whether hematopoietic cell MyD88 signaling contributed to inflammation and control of *B. melitensis* infection. To do this, we utilized mice that we previously generated that lack MyD88 signaling specifically in hematopoietic cells (MyD88$^{fl/fl\text{-}Vav1\text{-}cre}$) (25), along with MyD88$^{-/-}$ mice and control animals (wild type [WT] or MyD88$^{fl/fl}$). These mice were then footpad infected with 10^5 *B. melitensis* cells. The initiation of joint swelling was highly dependent on hematopoietic MyD88 signaling (Fig. 1A). This delayed initiation of joint swelling in mice lacking hematopoietic MyD88 was associated with decreased levels of proinflammatory cytokines (Fig. S2A to D) in the joint at day 2 postinfection. From day 6 postinfection onward, mice lacking hematopoietic MyD88 signaling had elevated joint swelling relative to control animals (Fig. 1A). While joint CFU levels were similar at day 2 postinfection, by day 7 postinfection mice lacking hematopoietic MyD88 had markedly higher joint *Brucella* burdens than did control animals (Fig. 1B). Hematopoietic MyD88 signaling appears to be critical regardless of the route of infection, as hematopoietic MyD88 contributed to control of *Brucella* infection in the spleen and liver 1 week after intraperitoneal (i.p.) challenge (Fig. S2E).

IFN-γ is not essential for MyD88-dependent protection against *B. melitensis* infection. Numerous studies (17, 19, 26), including our own (22), have found MyD88 protects the host against *Brucella* infection. While the protective function of MyD88

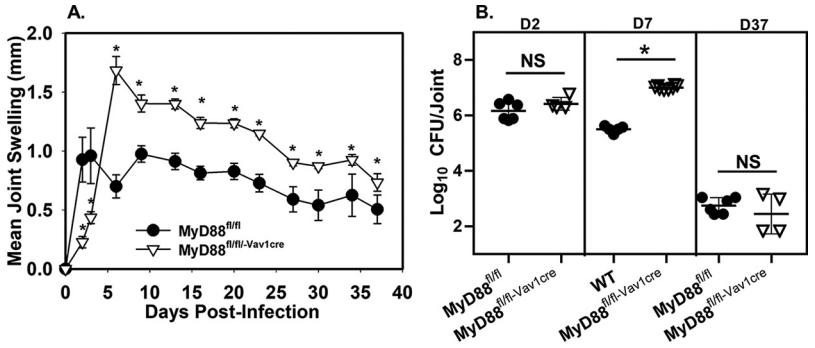

FIG 1 Hematopoietic MyD88 signaling mediates both inflammation and control of *Brucella* joint infection. (A) MyD88$^{fl/fl}$ (control) and hematopoietic MyD88-deficient (MyD88$^{fl/fl\text{-}Vav1cre}$) mice ($n = 4$ to 6/group) were infected in both rear footpads with 1×10^5 *B. melitensis* 16M, and joint swelling was measured over time. (B) MyD88$^{fl/fl\text{-}Vav1cre}$ or control animals (WT or MyD88$^{fl/fl}$) ($n = 4$ to 8/group) were infected in both rear footpads with 1×10^5 *B. melitensis* 16M, and colonization of the joint by *Brucella* was determined at 2, 7, or 37 days postinfection. *, $P < 0.05$ compared to control mice (WT or MyD88$^{fl/fl}$). Error bars depict standard deviations (SD) from the means. Data are representative of 2 independent experiments. ns, not significant.

has frequently been attributed to promotion of IFN-γ production (19), to our knowledge the role of IFN-γ in MyD88-dependent protection against *Brucella* has not been directly tested. During *B. melitensis*-induced arthritis, we found MyD88 was critical for early IFN-γ production in the joint; however, IFN-γ levels in MyD88$^{-/-}$ mice reached levels found in WT mice within a few days (22). To determine if the protective effect of MyD88 required IFN-γ, we treated footpad-infected WT and MyD88$^{-/-}$ mice with anti-IFN-γ antibodies and measured *B. melitensis* CFU numbers in joints. We found MyD88 protected against joint infection even in the absence of IFN-γ (Fig. 2A). We next infected mice systemically to determine if the IFN-γ-independent effect of MyD88 was specific to the route of challenge. Although *B. melitensis* infection is not lethal in MyD88$^{-/-}$ mice (17, 19, 26), we found MyD88$^{-/-}$ animals neutralized of IFN-γ succumb to infection following i.p. challenge with *B. melitensis*, while WT mice treated with anti-IFN-γ did not (Fig. 2B). In addition, MyD88$^{-/-}$ animals neutralized of IFN-γ succumbed more rapidly to infection than did IFN-$\gamma^{-/-}$ mice even when infected with a 100-fold lower dose of *B. melitensis* (Fig. S3A).

We also measured bacterial burdens in i.p. infected WT and MyD88$^{-/-}$ mice treated with anti-IFN-γ. For these studies, we utilized a lower infectious dose (10^3 CFU) in an

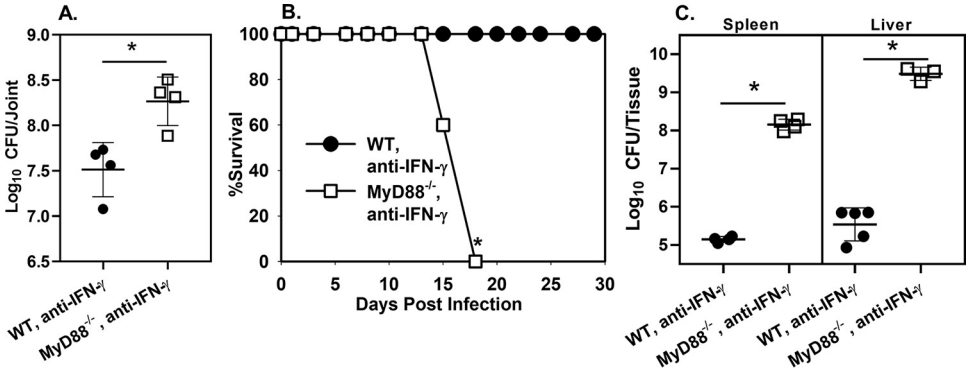

FIG 2 IFN-γ is not essential for MyD88-dependent protection against *Brucella* infection. (A) WT and MyD88$^{-/-}$ mice ($n = 4$) were treated with anti-IFN-γ and infected in both rear footpads with 1×10^5 *B. melitensis* 16M. Mice were euthanized at day 7, and joint CFU numbers were enumerated. (B) WT and MyD88$^{-/-}$ mice ($n = 5$) were treated with anti-IFN-γ and infected i.p. with 1×10^5 *B. melitensis* 16M. Survival was monitored over time. (C) WT and MyD88$^{-/-}$ mice ($n = 5$) were treated with anti-IFN-γ and infected i.p. with 1×10^3 *B. melitensis* 16M. CFU levels were measured in spleen and liver 16 days postinfection. Error bars depict SD from the mean. Data in panel A are from one experiment, while the data in panels B and C are representative of 2 independent experiments. *, $P < 0.05$ compared to WT, anti-IFN-γ-treated mice.

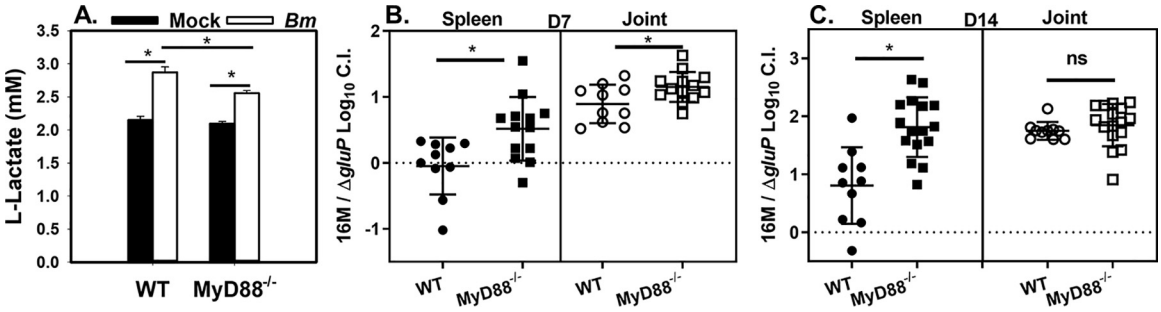

FIG 3 MyD88 deficiency impairs macrophage glycolysis and causes an enhanced reliance on *gluP* for *Brucella*-mediated virulence. (A) Macrophages from WT or MyD88$^{-/-}$ mice (n = 5 to 6 wells/group) were infected with *B. melitensis* 16M at an MOI of 100, and lactate levels in supernatants were measured 48 h postinfection. *, $P < 0.05$ as determined via ANOVA. (B and C) WT or MyD88$^{-/-}$ mice were footpad infected (n = 10 to 16) with 10^5 CFU containing a 1:1 mix of WT *B. melitensis* 16M and *B. melitensis* Δ*gluP* mutant. Seven (B) or 14 (C) days postinfection, a $\log_{10}$ competitive index (CI) was calculated for number of CFU recovered from spleens and joints. Error bars depict SD from the means. Data in panel A are representative of 2 independent experiments, while data in panels B and C are combined from two experiments. *, $P < 0.05$ compared to the CI in WT tissues in panels B and C.

attempt to extend the survival time of the animals. Strikingly, 16 days after i.p. infection, tissue *B. melitensis* burdens were up to 10,000-fold higher in anti-IFN-γ-treated MyD88$^{-/-}$ mice than in anti-IFN-γ-treated WT animals (Fig. 2C). Taken together, these data demonstrate that MyD88 signaling has protective effects against *Brucella* infection beyond enhancing IFN-γ production. MyD88 also promotes production of TNF-α (Fig. S2A), which we have found is critical for control of *Brucella* joint infection (Fig. S3B). However, TNF-α levels were similar in IFN-γ-neutralized, WT, and MyD88$^{-/-}$ joints from *Brucella*-infected mice (Fig. S3C). Therefore, the IFN-γ-independent protective effect of MyD88 does not appear to be TNF-α dependent.

MyD88 modulates macrophage metabolism *in vitro* and the requirement for *gluP*-mediated virulence *in vivo*. *B. abortus* preferentially replicates in alternatively activated macrophages (AAMs) during chronic splenic infection (27). AAMs generate energy via fatty acid oxidation, which results in increased intracellular glucose availability. Enhanced replication of *B. abortus* in AAMs requires utilization of host glucose mediated by the *Brucella* glucose transporter GluP (27). In contrast, TLR stimulation promotes host glycolysis and glucose consumption (20, 21). For this reason, we questioned whether MyD88-dependent host glycolysis could restrict glucose availability to control *B. melitensis* infection. First, we measured L-lactate as an output of glycolysis. While *B. melitensis* induced L-lactate production by both WT and MyD88$^{-/-}$ bone marrow-derived macrophages (BMDMs), MyD88$^{-/-}$ cells produced significantly less L-lactate than WT cells (Fig. 3A). To determine if MyD88-dependent glucose restriction could contribute to control of infection *in vivo*, we footpad infected WT and MyD88$^{-/-}$ mice with a 1:1 ratio of WT *B. melitensis* and a chloramphenicol-resistant *B. melitensis* Δ*gluP* mutant we generated. One and 2 weeks postinfection, tissue homogenates were plated onto regular agar and agar containing chloramphenicol to determine the ratio of WT *B. melitensis* to *B. melitensis* Δ*gluP* mutant. We then calculated a $\log_{10}$ competitive index (CI), where 0 indicates the mutant is not attenuated (dashed lines in Fig. 3B and C), while a CI of 1 indicates the mutant is attenuated 10-fold. *gluP* was required for *B. melitensis* virulence in WT spleens at 2 (Fig. 3C) but not at 1 week postinfection (Fig. 3B), which mimics findings in *B. abortus* where *gluP* was required for chronic splenic infection but was dispensable for spleen colonization early after infection (27, 28). Interestingly, the CI was significantly higher in spleens from MyD88$^{-/-}$ mice than from spleens from WT mice at both time points. In joints, *B. melitensis* Δ*gluP* mutant was attenuated in WT mice at both 1 and 2 weeks postinfection. At 1 week postinfection, *B. melitensis* Δ*gluP* mutant was also more highly attenuated in joints from MyD88$^{-/-}$ than from WT mice. When examining raw colony counts in tissues (for example, see Fig. S4A), it was also evident that WT *B. melitensis*, but not *B. melitensis* Δ*gluP* mutant, colonizes MyD88-deficient mice more efficiently than control animals. Collectively, these data indicate MyD88 deficiency causes an enhanced reliance on *gluP* for *Brucella*

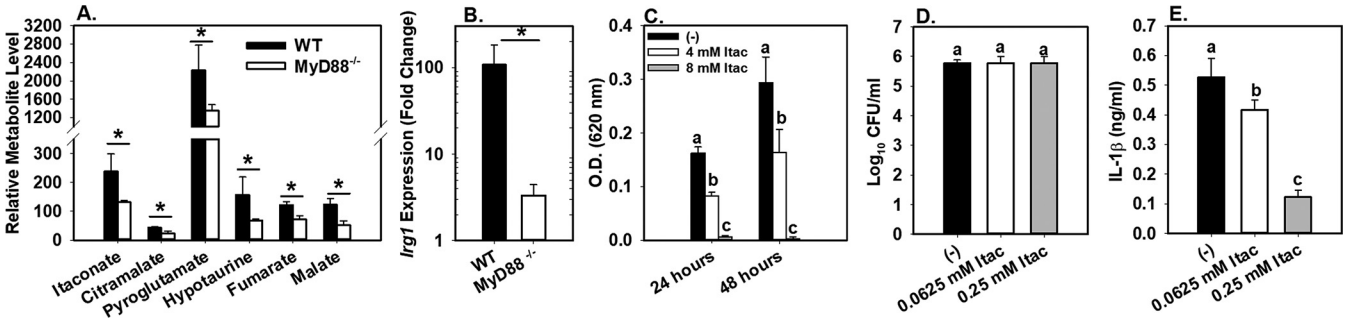

FIG 4 MyD88 is required for macrophage production of itaconate. (A) Macrophages from WT or MyD88$^{-/-}$ mice ($n = 4$ wells/group) were infected with *B. melitensis* 16M at an MOI of 100, and intracellular metabolite levels were determined via GC-MS at 48 h postinfection. (B) WT or MyD88$^{-/-}$ macrophages ($n = 4$ wells/group) were infected with *B. melitensis* 16M at an MOI of 100, and relative *Irg1* expression was determined at 6 h postinfection. (C) *Brucella* was cultured in broth ($n = 8$ wells/group) with or without exogenous itaconate, and growth was assessed by OD at 24 and 48 h postinfection. (D and E) WT macrophages ($n = 4$ wells/group) were infected with *B. melitensis* 16M at an MOI of 100. Some macrophages were also treated with dimethyl itaconate. Twenty-four hours postinfection, intracellular CFU numbers and IL-1β levels in supernatants were measured. Error bars depict SD from the mean. Data in panels A and B are from one experiment, while data in panels C to E are representative of 2 to 3 independent experiments. *, $P < 0.05$ compared to WT macrophages in panels A and B Sample means at the same time point with the same letter are not significantly different from each other via ANOVA in panels C to E. *, $P < 0.05$.

virulence and suggest that timing, the host tissue, and MyD88 signaling affect the metabolic requirements for *Brucella* virulence.

MyD88-dependent itaconate has antibacterial and immunomodulatory activities. As MyD88-dependent glucose restriction was important for control of *B. melitensis* infection *in vivo*, we next investigated the effect of MyD88 on other metabolite levels by nontargeted metabolite profiling of macrophages. BMDMs from WT and MyD88$^{-/-}$ mice were infected with *B. melitensis*. Forty-eight hours postinfection, polar metabolites were extracted from cell lysates with methanol, derivatized, and analyzed via gas chromatography-mass spectrometry (GC-MS). Over 100 metabolites were detected, and the expression level of 10 of these metabolites was altered $\geq$1.5-fold by MyD88 deficiency (Table S2). In particular, the expression levels of itaconate, citramalate, pyroglutamate, hypotaurine, fumarate, and malate were all significantly decreased in the absence of MyD88 (Fig. 4A).

Of particular interest was the regulation of itaconate by MyD88. Itaconate has been shown to have antibacterial effects (29–31). The *Irg1* gene encodes aconitate decarboxylase, which generates itaconate from aconitate (29). We found *Irg1* to be upregulated ~100-fold in *B. melitensis*-infected macrophages in a MyD88-dependent manner (Fig. 4B). This induction of *Irg1* by *B. melitensis* mirrors other reports in which *Irg1* was shown to be one of the most highly upregulated genes in *B. abortus*-infected macrophages (32). Activated macrophages produce up to 8 mM intracellular itaconate, but it is thought higher levels can accumulate in specific compartments (31). Here, itaconate levels of 4 to 8 mM caused a dose-dependent inhibition of *B. melitensis* growth in broth (Fig. 4C). The antibacterial effect of itaconate has been suggested to be pH dependent, because at low pH itaconate can transverse the bacterial membrane (33). However, the effect of itaconate on *Brucella* growth does not appear to be due solely to lowering of pH, as *B. melitensis* grew significantly better in broth adjusted to a pH of 5.0 with HCl than in broth containing 8 mM itaconate (pH 5.0) (Fig. S4B).

In addition to antibacterial effects, itaconate can inhibit succinate dehydrogenase (SDH) in macrophages and cause succinate accumulation (34, 35). Indeed, we found itaconate levels appear to correlate with succinate levels in WT but not MyD88$^{-/-}$ cells (Fig. S4C and D). Itaconate-mediated inhibition of succinate oxidation by SDH can suppress macrophage mitochondrial respiration/reactive oxygen species (ROS) production and cytokine production (34, 35). To determine if itaconate can regulate cytokine production during *B. melitensis* infection, we treated BMDMs with 0.0625 or 0.25 mM dimethyl itaconate, a nonionic membrane-permeable form of itaconate (34) after *B. melitensis* infection. At these concentrations, dimethyl itaconate treatment suppressed IL-1β production by BMDMs in a dose-dependent manner without affecting intracellular

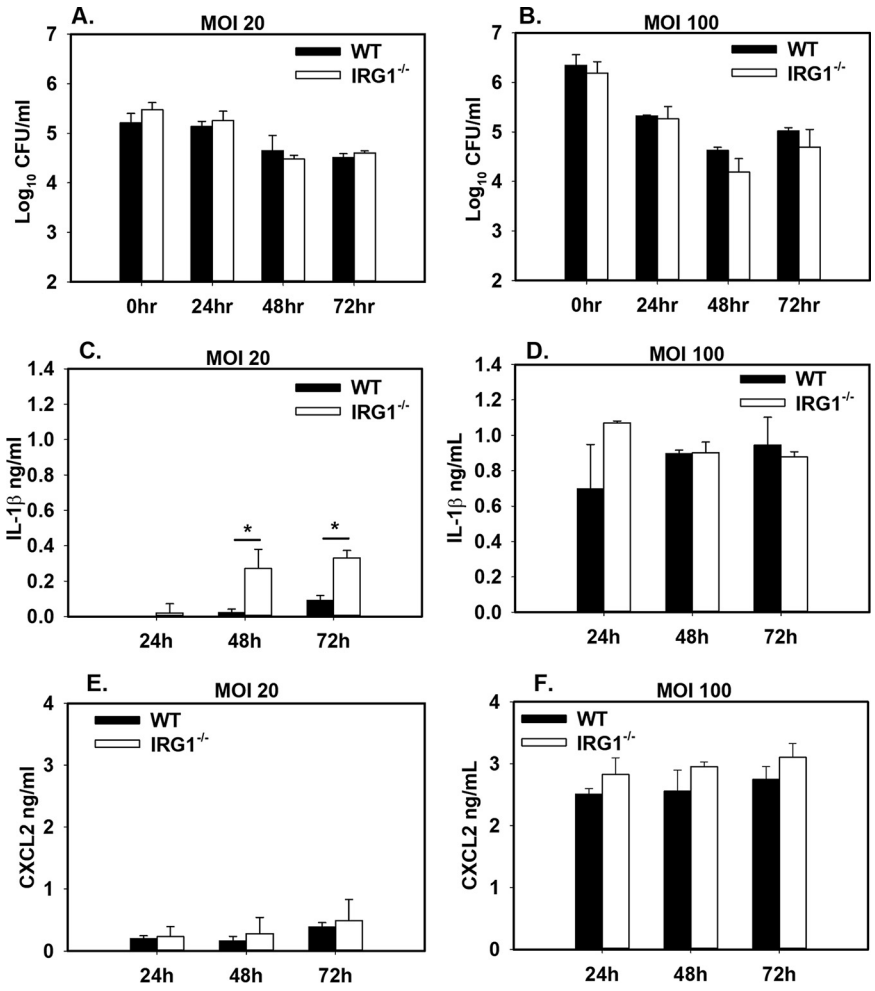

FIG 5 *Irg1* is dispensable for macrophage control of *Brucella* infection. (A to F) Macrophages from WT and IRG1$^{-/-}$ mice (n = 3 wells/group) were infected with *B. melitensis* 16M at an MOI of 20 or 100. At various time points after infection, intracellular CFU levels were determined (A and B), and IL-1β (C and D) and CXCL2 (E and F) were measured in supernatants. Error bars depict SD from the means. Data are representative of 3 independent experiments. *, $P < 0.05$ compared to WT macrophages.

B. melitensis levels (Fig. 4D, and E). Collectively, these data show itaconate can both inhibit the growth of *B. melitensis* and regulate macrophage cytokine production during *B. melitensis* infection.

***Irg1* contributes to control of *B. melitensis* following pulmonary infection.** We next investigated whether *Irg1*/itaconate contributed to control of *Brucella* infection. First, we infected WT and IRG1$^{-/-}$ BMDMs with *B. melitensis*. We measured intracellular bacterial burdens at 0, 24, 48, and 72 h postinfection but did not see any striking differences between WT and IRG1$^{-/-}$ cells (Fig. 5A and B). As we found that exogenous itaconate suppressed *Brucella*-induced IL-1β production by macrophages (Fig. 4E), we also measured cytokine production in supernatants from WT and IRG1$^{-/-}$ BMDMs. *Irg1* deficiency enhanced IL-1β production when macrophages were infected at a multiplicity of infection (MOI) of 20 but not at an MOI of 100 (Fig. 5C and D). In response to *Mycobacterium tuberculosis*, *Irg1* regulates CXCL2 expression (29) and the receptor for CXCL2 mediates *Brucella*-induced arthritis (36). However, we did not find CXCL2 levels in *Brucella*-infected macrophages to be altered by *Irg1* (Fig. 5E and F).

While *Irg1* deficiency did not alter control of *B. melitensis* infection in macrophages, others have shown that during *M. tuberculosis* infection *Irg1* contributes to control of infection *in vivo* but not *in vitro* (29). To determine whether *Irg1* contributes to the control of *B. melitensis in vivo*, we footpad infected WT and IRG1$^{-/-}$ mice and measured

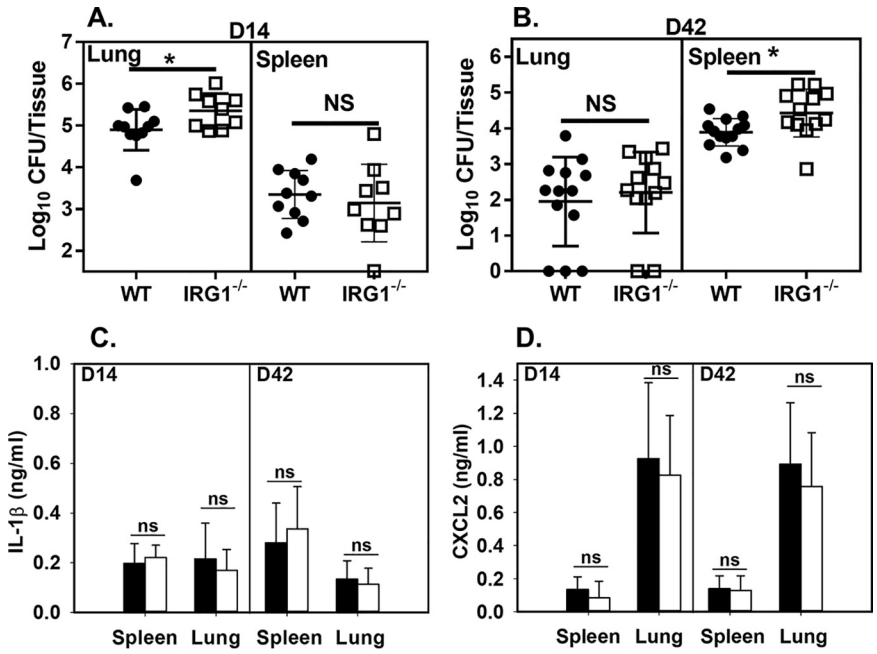

FIG 6 *Irg1*-deficient mice display enhanced susceptibility to pulmonary challenge with *Brucella*. (A to D) WT or IRG1$^{-/-}$ mice ($n = 9$ to 12/group) were infected i.n. with 1×10^5 CFU of *B. melitensis* 16M. Fourteen (D14) or 42 (D42) days postinfection, CFU (A and B), IL-1β (C), and CXCL2 (D) levels were measured in lung and spleen. Error bars depict SD from the means. Data are combined from 2 experiments. *, $P < 0.05$ compared to WT tissues.

Brucella levels in joints 1 and 2 weeks postinfection. At these time points, *Irg1* deficiency did not markedly alter joint *Brucella* burdens (Fig. S5A). There have been limited studies that have shown that *Irg1* contributes to control of bacterial infection *in vivo*. Of particular interest were reports that mice lacking *Irg1* are more susceptible to pulmonary infection with *M. tuberculosis* (29) and the live vaccine strain of *Francisella tularensis* (37). As *Brucella* can be acquired via the respiratory route, we next tested the ability of WT and IRG1$^{-/-}$ mice to control pulmonary infection with *B. melitensis*. At 2 weeks postinfection, *Irg1* deficiency led to an increase in the amount of *Brucella* recovered from the lung but not the spleen (Fig. 6A). During *M. tuberculosis* infection, *Irg1* plays a greater role in chronic than in acute infection. Therefore, we measured *Brucella* counts 6 weeks after pulmonary infection. At this time point, we found that *Irg1* deficiency impaired resistance to colonization of the spleen but not the lung (Fig. 6B). While *Irg1*/itaconate regulated IL-1β production *in vitro* (Fig. 4 and 5), we found that IL-1β and CXCL2 levels were similar in WT and IRG1$^{-/-}$ mice following pulmonary infection (Fig. 6C and D). In sum, *Irg1*/itaconate appears to have a route-dependent role in controlling *Brucella* infection *in vivo*.

DISCUSSION

Brucella has long been known to infect a variety of phagocytic and nonphagocytic cells. Here, we too found that *Brucella* infects both hematopoietic and nonhematopoietic cells within the joints of mice (see Fig. S1 in the supplemental material). However, by using conditional knockout mice, we showed that the protective effect of MyD88 against *Brucella* infection is mediated by cells of the hematopoietic lineage (Fig. 1). In the future, we will determine the function of specific hematopoietic subsets on MyD88-dependent control of infection. Due to the role of MyD88 in promoting cytokine production and glycolysis in myeloid cells, macrophages and neutrophils appear to be cell types respond to *Brucella* via MyD88. However, MyD88 is also involved in T cell activation and, in particular, can mediate IFN-γ production by T cells in response to IL-18 (38). Indeed, others have shown that mice with a T cell-specific

MyD88 deficiency are more susceptible to *B. abortus* infection (38), which suggests that T cell MyD88 signaling contributes in part to the protective effect of hematopoietic MyD88 that we demonstrated here.

Previously, we showed that the protective effect of MyD88 against *Francisella tularensis* was IFN-γ dependent (25). As we and others have found that MyD88 signaling promotes IFN-γ production during experimental brucellosis (17, 22, 26), we sought to directly investigate the role of IFN-γ in MyD88-dependent protection against *Brucella*. Surprisingly, we found that even in the absence of IFN-γ, MyD88 contributed to protection against colonization of the joint and other tissues by *Brucella*. MyD88-deficient mice neutralized of IFN-γ also succumbed to infection while WT mice treated with anti-IFN-γ did not (Fig. 3B). Collectively, these data indicate that while MyD88 promotes IFN-γ production, IFN-γ is not solely responsible for the protective effect of MyD88 against *Brucella* infection.

The glucose transporter, GluP, is essential for *B. abortus* to exploit the increased availability of glucose present in alternatively activated macrophages (27). To our knowledge, *gluP* has not been investigated in *B. melitensis*. Thus, we created a *B. melitensis* 16M strain lacking *gluP*. As shown for *B. abortus* (27), supplementation of broth with glucose enhances the growth of wild-type *B. melitensis* (Fig. S5B). In contrast, a *B. melitensis* Δ*gluP* mutant showed no significant difference in growth upon glucose supplementation, while complementation of *gluP* restored the ability of the mutant to utilize glucose (Fig. S5B). These results show that *gluP* is important for the utilization of glucose by *B. melitensis*.

In vitro, we found that MyD88 deficiency impaired macrophage glycolysis (Fig. 3A). We therefore performed *in vivo* experiments to determine if MyD88 deficiency enhanced glucose availability which, in turn, would cause an increased reliance on GluP for *Brucella* virulence. Indeed, we found that *B. melitensis* Δ*gluP* mutant was more highly attenuated in tissues of MyD88$^{-/-}$ mice than in tissues from wild-type animals (Fig. 3B and C). In addition to promoting host cell glycolysis, MyD88 signaling also induces cytokine production, which likely affects cellular recruitment and the composition of *Brucella*-infected tissues. Therefore, in the future we will perform *in vivo* studies to confirm that host cell-intrinsic MyD88-dependent changes in glycolysis result in an enhanced role for *gluP* in *Brucella* virulence. As *gluP* appears to be more important for *Brucella* colonization of the joint than the spleen in the first 2 weeks after infection (Fig. 3B and C), we will also further investigate the tissue-specific role of *gluP* on *Brucella* virulence. For example, alveolar macrophages (AMs) are a major reservoir known to support *Brucella* replication following pulmonary infection (39). Interestingly, AM metabolism is skewed toward fatty acid oxidation, while monocyte-derived interstitial macrophages are more glycolytic (40). With this in mind, we infected mice intranasally (i.n.) with a 1:1 ratio of WT *B. melitensis* and *B. melitensis* Δ*gluP* mutant and measured the relative colonization of the lung at 1 week postinfection. Interestingly, we found that the *B. melitensis* Δ*gluP* mutant was attenuated in the lung ~20-fold (Fig. S5C), perhaps due to an inability to exploit the available glucose in AMs.

Next, we investigated whether other metabolites regulated by MyD88 signaling could contribute to control of *Brucella* infection. Via GC-MS, we found that the production of several metabolites was impaired in MyD88-deficient macrophages infected with *B. melitensis* (Fig. 4A). Here, we focused on itaconate due to its known antibacterial and immunomodulatory effects in response to other infections (29–31). We found that 4 to 8 mM itaconate was able to restrict *Brucella* growth in broth (Fig. 4C). Similar to what we found with *Brucella*, 10 mM itaconate has activity against *Legionella pneumophila* and *Salmonella enterica*, while a higher itaconate concentration (25 mM) is required to restrict growth of *M. tuberculosis* (30, 31). Exogenous itaconate also regulated cytokine production by *Brucella*-infected macrophages (Fig. 4C to E). *In vitro*, *Irg1* deficiency did not affect macrophage control of *Brucella* but did have an MOI-dependent effect on IL-1β production (Fig. 5).

While *Irg1*-deficient macrophages were not impaired in their ability to control *B. melitensis in vitro*, we did find slightly, but significantly, higher bacterial loads in tissues

from IRG1$^{-/-}$ mice than from control animals following pulmonary infection. *B. melitensis* does encode a cluster of genes (BMEII1074-1076) with sequence similarity to a *Pseudomonas aeruginosa* operon that mediates degradation of itaconate (41). Therefore, breakdown of itaconate by this *Brucella* gene cluster could explain the limited effect of *Irg1*/itaconate on control of infection. In addition, the suppressive effect of *Irg1*/itaconate on production of IL-1 (Fig. 4 and 5), which we have shown to be protective against *Brucella* (42), could also moderate the ability of *Irg1*/itaconate to restrict infection. While the effect of *Irg1* was modest, in other systems *Irg1* and nitric oxide have redundant effects on control of bacterial infection (43). We (24) and others (26) have shown that nitric oxide contributes modestly to control of *Brucella* infection. Therefore, it is possible that nitric oxide and itaconate have redundant effects on restriction of *Brucella* infection. Future studies will explore this possibility.

In addition to direct antibacterial effects, itaconate also inhibits bacterial isocitrate lyase enzymes (ICLs) involved in the bacterial glyoxylate shunt (31). ICLs can be important for the growth of bacteria generating energy via β-oxidation of fatty acids (29, 30, 44). *Brucella* has an intact glyoxylate shunt, and the ICL, AceA, has been purported to be important for the virulence of *B. suis* (45), but not *B. abortus* (46). The role of AceA in the virulence of *B. melitensis* is unknown; therefore, in the future we will determine how interactions between itaconate and AceA affect the outcome of *B. melitensis* infection.

In conclusion, we show here that hematopoietic MyD88 signaling mediates control of *Brucella* infection and that the protective effect of MyD88 is not entirely dependent on IFN-γ. In addition, we show that MyD88 has multiple effects on host metabolism that contribute to control of *Brucella* infection as detailed in our working model (Fig. S6). Like *Brucella*, *Salmonella* also exploits host glucose to cause a persistent infection (47). Therefore, MyD88-dependent glucose consumption may be a mechanism by which host cells are protected from a variety of infections. Lastly, we show that *Irg1*/itaconate can restrict *Brucella* infection and regulate proinflammatory cytokine responses. As *Irg1*/itaconate can restrict *Brucella* infection while at the same time dampen inflammatory responses, exogenous itaconate treatment has potential as a complement to antibiotic therapy of brucellosis.

MATERIALS AND METHODS

Bacterial strains and growth conditions. All experiments with live *Brucella melitensis* were performed in biosafety level 3 (BSL-3) facilities. *B. melitensis* 16M, obtained from Montana State University (Bozeman, Montana), was grown on *Brucella* agar (Ba) at 37°C (Becton, Dickinson, Franklin Lakes, NJ). Colonies were picked from Ba plates, and strains were cultured in *Brucella* broth (Bb; Becton, Dickinson) overnight at 37°C with shaking. The overnight *Brucella* concentration was estimated by measuring the optical density (OD) at 600 nm, and the inoculum was diluted to the appropriate concentration in sterile phosphate-buffered saline (sPBS). Actual viable titer was confirmed by serial dilution of the *B. melitensis* inoculum onto Ba plates.

Mice. Experiments were conducted using 6- to 12-week-old age- and sex-matched mice on a C57BL/6J background. C57BL/6J, MyD88$^{-/-}$, IFN-$\gamma^{-/-}$, and IRG1$^{-/-}$ mice were obtained from Jackson Laboratory (Bar Harbor, ME). To generate mice with a hematopoietic-specific MyD88 deficiency, mice with floxed MyD88 alleles (stock number 008888, MyD88$^{fl/fl}$; Jackson) and mice expressing cre recombinase under the control of the Vav1 (stock number 008610; Jackson) promoter were intercrossed as previously described (25). Wild-type (WT) C57BL/6 and MyD88$^{fl/fl}$ mice displayed a similar phenotype following infection and were used interchangeably as control animals as described in the legends of Fig. 1 and Fig. S2 in the supplemental material. For footpad infection, mice were infected in both rear footpads with 50 μl of PBS containing 1×10^5 CFU of *Brucella* (22). Ankle swelling was evaluated in relation to basal joint measurements made prior to infection, as described previously (22). Ankle swelling was measured at various time points by collective measurements of both tibiotarsal joints. The difference of the recorded measurement from the basal measurement was reported as mean joint swelling. Intraperitoneal (i.p.) infections were performed by injecting 1×10^5 CFU of *Brucella* in 200 μl of PBS (36). For intranasal (i.n.) infections, mice were first anesthetized with 100 mg/kg of body weight ketamine and 10 mg/kg xylazine, and 20 μl of PBS containing 1×10^5 CFU of *Brucella* was placed onto the anterior nares. To neutralize IFN-γ during footpad infection, mice were treated i.p. with 0.5 mg anti-IFN-γ (clone XMG1.2; BioXCell, Lebanon, NH) 1 day prior to and 3 days after infection (24). To neutralize IFN-γ during i.p. infection, mice were treated i.p. with 0.25 mg anti-IFN-γ 1 day prior to infection and 3 times a week thereafter (36). To neutralize TNF-α, mice were given 0.5 mg of anti-TNF-α (clone XT3.11; BioXCell) 1 day prior to and 3 days after infection (48). Control mice received Rat IgG (Southern Biotech, Birmingham,

AL). All studies were conducted in accordance with the University of Missouri Animal Care and Use Committee guidelines.

Generation and complementation of *B. melitensis* Δ*gluP* mutant. The *gluP* (BMEII1053) gene in *B. melitensis* 16M was replaced in frame with a chloramphenicol resistance gene (*catR*) from plasmid pKD3 (49) using the suicide plasmid pNTPS139 (50). Approximately 1,000-bp fragments upstream and downstream of *gluP* were amplified by PCR using primers shown in Table S1. We also generated a 1,044-bp fragment containing the *catR* gene from pKD3 using primers listed in Table S1. The 5′ end of the forward primer used to amplify the upstream fragment of *gluP* contained homology to 30 bp upstream of the BamHI site in pNTPS139. The 5′ end of the forward primer used to amplify the *catR* gene from pKD3 contained 30 bp homologous to the 3′ end of the upstream *gluP* fragment. The downstream fragment of *gluP* was amplified using a forward primer whose 5′ end contained 30 bp homologous to the 3′ end of the *catR* fragment, while the 5′ end of the downstream *gluP* fragment reverse primer contained 30 bp homologous to the 30 bp downstream of the SalI site of pNTPS139. pNTPS139 was digested with BamHI/SalI. The upstream *gluP* and *catR* and downstream *gluP* fragments, along with BamHI/SalI-digested pNPTS139, were all ligated together using the NEB Hi-Fi DNA assembly kit according to the manufacturer's instructions (New England Biolabs, Ipswich, MA). This plasmid was then introduced into *B. melitensis* 16M, and merodiploid transformants were obtained by selection on Ba plus 25 μg/ml kanamycin. A single kanamycin-resistant clone was grown overnight in Bb and then plated onto Ba containing 10% sucrose. Genomic DNA from sucrose-resistant, kanamycin-sensitive colonies was isolated and screened by PCR for replacement of the gene of interest. To complement the *gluP* deletion strain, the *gluP* gene plus ~500 bp upstream and downstream were amplified with primers gluP-recon-F and gluP-recon-R (Table S1), cloned using the Hi-Fi assembly kit into pNPTS139, and restored at the native site (51) using the two-step recombination strategy outlined above.

Effect of glucose and itaconate on growth of *Brucella in vitro*. *B. melitensis* 16M, an isogenic *gluP* mutant (*B. melitensis* Δ*gluP* mutant), and a complemented mutant (*B. melitensis* Δ*gluP*′ mutant) were grown for 18 h in Bb, centrifuged, and then washed with sPBS three times. The OD at 600 nm was adjusted to 1.0 in PBS, and the bacteria were then diluted 1:100 into Luria-Bertani broth (LB; Becton, Dickinson) or LB containing 0.05% glucose. The samples were placed in a 96-well plate and incubated at 37°C and 5% CO_2. The final OD was measured 48 h postinoculation in a plate reader at 620 nm. To determine the effect of itaconate on growth, *B. melitensis* 16M was grown overnight in Bb as explained above. The OD of *B. melitensis* was adjusted to 0.01, and the cultures were grown in Bb containing 0, 4, or 8 mM itaconic acid (AdipoGen Life Sciences, San Diego, CA). The samples were cultured in a 96-well plate and incubated for 24 to 48 h at 37°C and 5% CO_2, and the OD at 620 nm was read as explained above.

Measurement of bacterial burdens and cytokines in tissues. At various times after infection, mice were euthanized, and spleens, livers, lungs, or joints (following removal of skin) were harvested. Tissues were homogenized mechanically in sPBS (22). A series of 10-fold dilutions were performed in triplicate in sPBS and plated onto Ba. Plates were incubated 3 to 4 days at 37°C and 5% CO_2, colonies were enumerated, and the number of CFU/tissue was calculated. For *in vivo* competition experiments, mice were infected with an inoculum containing a 1:1 ratio of wild-type *B. melitensis* and *B. melitensis* Δ*gluP* mutant. The titer of this inoculum was determined at the time of infection by plating on regular Ba and Ba containing 5 μg/ml chloramphenicol. After infection with the 1:1 mixture of wild-type *B. melitensis* and *B. melitensis* Δ*gluP* mutant, murine tissues were homogenized and plated onto both regular Ba and Ba with chloramphenicol to determine the ratio of wild-type to Δ*gluP* mutant *Brucella*. A $\log_{10}$ competitive index (where 0 indicates the mutant is not attenuated) was then calculated based on the ratio of the recovery of the two strains in tissues relative to their ratio in the inoculum. For measurement of cytokines, homogenized tissues were centrifuged at 2,000 × *g* for 5 min, and supernatants were filter sterilized (0.2 μm) and stored at −70°C prior to analysis. The data shown in Fig. 6 were obtained by enzyme-linked immunosorbent assay (ELISA) using a mouse IL-1β ELISA Ready Set Go kit (Invitrogen, Carlsbad, CA) and a mouse CXCL2/MIP-2 DuoSet ELISA kit (R&D Systems, Minneapolis, MN) according to the manufacturers' instructions. The cytokine data in Fig. S2A to D and S3B were obtained with a Luminex (Austin, TX) MagPix instrument using Milliplex magnetic reagents according to the manufacturer's instructions (MilliporeSigma, Burlington, MA). Luminex data were analyzed with Milliplex Analyst software (MilliporeSigma).

Macrophage generation and infections. Bone marrow-derived macrophages (BMDMs) were generated and infected as described previously (52). Bone marrow was flushed from the femurs and tibias of mice and then cultured in complete medium (CM; RPMI 1640, 10% fetal bovine serum [FBS], 10 mM HEPES buffer, 10 mM nonessential amino acids, 10 mM sodium pyruvate) containing 30 ng/ml recombinant murine macrophage colony-stimulating factor (M-CSF; Shenandoah Biotechnology, Warwick, PA). After 3 to 4 days of culture, fresh CM containing 30 ng/ml M-CSF was added to culture flasks. Adherent cells were then collected at 6 to 7 days after bone marrow harvest by adding 0.05% trypsin (MilliporeSigma). Cells were plated at 1×10^6 cells/ml in fresh CM and left to adhere overnight. Cells were infected at a multiplicity of infection (MOI) of 20 or 100 *B. melitensis* 16M as described in the figure legends. Cells were infected for 6 h, washed with sPBS, and then cultured in CM containing 50 μg/ml gentamicin for 30 min. Cells were then washed with sPBS and left to incubate in CM containing 2.5 μg/ml gentamicin for the remainder of the experiment. This time is considered 0 h postinfection. At this time, 0.0625 to 0.25 mM 4-dimethyl itaconate (Acros, Fair Lawn, NJ) was added to some cultures (34). At 0, 24, 48, or 72 h postinfection, supernatants were harvested and macrophages were washed and then lysed. These lysates were plated on Ba to determine the amount of intracellular *Brucella*. Supernatants were used for L-lactate quantification as described below. Measurements of IL-1β or CXCL2 were obtained by ELISA as described above.

Lactic acid quantification in cell culture supernatants. BMDM supernatants were centrifuged at 13,000 × *g* for 10 min to remove cell debris. Supernatants were then deproteinated using a Vivaspin 500

10K molecular weight cutoff filter (Fisher Scientific, Waltham, MA) according to the manufacturer's instructions. L-Lactate was measured using the L-lactate kit (Eton Biosciences, San Diego, CA) according to the manufacturer's instructions.

Metabolite quantification by GC-MS. BMDMs were infected as described above. Forty-eight hours postinfection, supernatants were removed and cells were washed with sPBS and then lysed in H_2O. Cell lysates were then reconstituted to a final concentration of 80% methanol and transferred to glass vials. Lysates were dried overnight, resuspended in a solution containing 15 μg/ml ribitol (internal standard), vortexed, incubated at 50°C for 1 h, dried, reconstituted in 50 μl of pyridine containing fresh 15 mg/ml methoxyamine-HCl, sonicated for 10 min, vortexed, and placed in a 50°C oven for 1 h. Samples were allowed to equilibrate to room temperature and then 50 μl of *N*-methyltrimethylsilyltrifluoroacetamide plus 1% trimethylchlorosilane (Fisher Scientific) was added. Samples were vortexed, incubated for 1 h at 50°C, centrifuged, and transferred to glass inserts for injection. Samples were analyzed using GC-MS on an Agilent 6890 GC coupled to a 5973N MSD mass spectrometer with a scan range from *m/z* 50 to 650. Separations were performed by using a 60-m DB-5MS column (0.25-mm inner diameter, 0.25-μm film thickness; J&W Scientific) and a constant flow of 1.0 ml/min helium gas at the University of Missouri Metabolomics Center. Results were interpreted using MetaboAnalyst software (https://www.metaboanalyst.ca/) (53) with a fold change cutoff of 1.5 and a *P* value threshold of 0.05.

Flow cytometry. Rear ankle joints were processed with collagenase/DNase as described previously (52), and cells were acquired on a CyAn ADP analyzer or sorted on a MoFlo XDP (Beckman Coulter, Brea, CA). FlowJo (Tree Star, Ashland, OR) software was used for analysis. Immunofluorescence staining was performed using the following fluorochrome-labeled monoclonal antibodies from eBioscience (San Diego, CA): F4/80 (BM8), Ly-6G (1A8), and CD45.2 (104). Cells were sorted and gated as $CD45.2^-$ (nonhematopoietic), $CD45.2^+/F4/80^+/Ly\text{-}6G^-$ (macrophages), $CD45.2^+/F4/80\text{-}/Ly\text{-}6G^{HI}$ (neutrophils), and $CD45.2^+/F4/80\text{-}/Ly\text{-}6G^-$ (other hematopoietic/$CD45.2^+$).

Quantitative RT-PCR. Macrophages were infected with *B. melitensis* as described above. RNA was isolated from cell lysates using the Qiagen RNeasy kit (Valencia, CA, USA). cDNA was generated using the Superscript III first-strand synthesis system (Invitrogen, Carlsbad, CA) using oligo(dT) primers. The quantitative reverse transcriptase PCR (RT-PCR) was set up in duplicate, and data were collected on an Applied Biosystems StepOnePlus real-time PCR system (Foster City, CA, USA). Relative *Irg1* mRNA in relation to glyceraldehyde-3-phosphate dehydrogenase (GAPDH) was quantified by measuring SYBR green (Fisher Scientific) incorporation (54). Primers used are shown in Table S1.

Statistical analysis. Statistical analysis of the difference between two mean values was conducted using a two-tailed Student's *t* test with significance set at a *P* value of $\leq$0.05, while comparisons of $\geq$3 mean values were done using analysis of variance (ANOVA) followed by Tukey's test, with significance set at a *P* value of $\leq$0.05. Statistical significance of survival studies was determined using log-rank analysis with significance set at $\leq$0.05.

SUPPLEMENTAL MATERIAL

Supplemental material is available online only.

SUPPLEMENTAL FILE 1, PDF file, 0.5 MB.

SUPPLEMENTAL FILE 2, XLSX file, 0.02 MB.

ACKNOWLEDGMENTS

This work was supported in part by the National Institutes of Health (NIH R21AI146397) and a pilot grant from the University of Missouri Metabolomics Center.

Carolyn A. Lacey is now employed by AbbVie. This article is composed of the authors' work and ideas and does not reflect the ideas of AbbVie. The remaining authors declare that the research was constructed in the absence of any commercial or financial relationships that could be construed as a potential conflict of interest.

REFERENCES

1. Hull NC, Schumaker BA. 2018. Comparisons of brucellosis between human and veterinary medicine. Infect Ecol Epidemiol 8:1500846. https://doi.org/10.1080/20008686.2018.1500846.
2. Zinsstag J, Roth F, Orkhon D, Chimed-Ochir G, Nansalmaa M, Kolar J, Vounatsou P. 2005. A model of animal-human brucellosis transmission in Mongolia. Prev Vet Med 69:77–95. https://doi.org/10.1016/j.prevetmed.2005.01.017.
3. Kaufmann AF, Fox MD, Boyce JM, Anderson DC, Potter ME, Martone WJ, Patton CM. 1980. Airborne spread of brucellosis. Ann N Y Acad Sci 353:105–114. https://doi.org/10.1111/j.1749-6632.1980.tb18912.x.
4. European Food Safety Agency, European Centre for Disease Prevention and Control. 2021. The European Union One Health 2019 zoonoses report. EFSA J 19:e06406. https://doi.org/10.2903/j.efsa.2021.6406.
5. Erbay A, Bodur H, Akinci E, Baştuğ A, Cevik MA. 2009. Brucellosis mimicking enteric fever. J Infect Dev Ctries 3:239–240.
6. Rajapakse CN. 1995. Bacterial infections: osteoarticular brucellosis. Baillieres Clin Rheumatol 9:161–177. https://doi.org/10.1016/s0950-3579(05)80153-0.
7. Gotuzzo E, Alarcon GS, Bocanegra TS, Carrillo C, Guerra JC, Rolando I, Espinoza LR. 1982. Articular involvement in human brucellosis: a retrospective analysis of 304 cases. Semin Arthritis Rheum 12:245–255. https://doi.org/10.1016/0049-0172(82)90064-6.
8. Ayaşlıoğlu E, Özlük Ö, Kılıç D, Kaygusuz S, Kara S, Aydın G, Çokca F, Tekeli E. 2005. A case of brucellar septic arthritis of the knee with a prolonged clinical course. Rheumatol Int 25:69–71. https://doi.org/10.1007/s00296-004-0453-1.
9. Adachi O, Kawai T, Takeda K, Matsumoto M, Tsutsui H, Sakagami M, Nakanishi K, Akira S. 1998. Targeted disruption of the MyD88 gene results in loss of IL-1- and IL-18-mediated function. Immunity 9:143–150. https://doi.org/10.1016/s1074-7613(00)80596-8.
10. Miller LS, O'Connell RM, Gutierrez MA, Pietras EM, Shahangian A, Gross CE, Thirumala A, Cheung AL, Cheng G, Modlin RL. 2006. MyD88 mediates

neutrophil recruitment initiated by IL-1R but not TLR2 activation in immunity against *Staphylococcus aureus*. Immunity 24:79–91. https://doi.org/10.1016/j.immuni.2005.11.011.
11. Gomes MT, Campos PC, Pereira GDS, Bartholomeu DC, Splitter G, Oliveira SC. 2016. TLR9 is required for MAPK/NF-kappaB activation but does not cooperate with TLR2 or TLR6 to induce host resistance to *Brucella abortus*. J Leukoc Biol 99:771–780. https://doi.org/10.1189/jlb.4A0815-346R.
12. Ferrero MC, Hielpos MS, Carvalho NB, Barrionuevo P, Corsetti PP, Giambartolomei GH, Oliveira SC, Baldi PC. 2014. Key role of Toll-like receptor 2 in the inflammatory response and major histocompatibility complex class ii downregulation in *Brucella abortus*-infected alveolar macrophages. Infect Immun 82:626–639. https://doi.org/10.1128/IAI.01237-13.
13. de Almeida LA, Macedo GC, Marinho FA, Gomes MT, Corsetti PP, Silva AM, Cassataro J, Giambartolomei GH, Oliveira SC. 2013. Toll-like receptor 6 plays an important role in host innate resistance to *Brucella abortus* infection in mice. Infect Immun 81:1654–1662. https://doi.org/10.1128/IAI.01356-12.
14. Campos MA, Rosinha GM, Almeida IC, Salgueiro XS, Jarvis BW, Splitter GA, Qureshi N, Bruna-Romero O, Gazzinelli RT, Oliveira SC. 2004. Role of Toll-like receptor 4 in induction of cell-mediated immunity and resistance to *Brucella abortus* infection in mice. Infect Immun 72:176–186. https://doi.org/10.1128/IAI.72.1.176-186.2004.
15. Vieira ALS, Silva TM, Mol JP, Oliveira SC, Santos RL, Paixão TA. 2013. MyD88 and TLR9 are required for early control of *Brucella ovis* infection in mice. Res Vet Sci 94:399–405. https://doi.org/10.1016/j.rvsc.2012.10.028.
16. Kawai T, Akira S. 2005. Toll-like receptor downstream signaling. Arthritis Res Ther 7:12–19. https://doi.org/10.1186/ar1469.
17. Macedo GC, Magnani DM, Carvalho NB, Bruna-Romero O, Gazzinelli RT, Oliveira SC. 2008. Central role of MyD88-dependent dendritic cell maturation and proinflammatory cytokine production to control *Brucella abortus* infection. J Immunol 180:1080–1087. https://doi.org/10.4049/jimmunol.180.2.1080.
18. Pasquali P, Adone R, Gasbarre LC, Pistoia C, Ciuchini F. 2002. Effect of exogenous interleukin-18 (IL-18) and IL-12 in the course of *Brucella abortus* 2308 infection in mice. Clin Diagn Lab Immunol 9:491–492. https://doi.org/10.1128/cdli.9.2.491-492.2002.
19. Gomes MT, Campos PC, Oliveira FS, Corsetti PP, Bortoluci KR, Cunha LD, Zamboni DS, Oliveira SC. 2013. Critical role of ASC inflammasomes and bacterial type IV secretion system in caspase-1 activation and host innate resistance to *Brucella abortus* infection. J Immunol 190:3629–3638. https://doi.org/10.4049/jimmunol.1202817.
20. Lachmandas E, Boutens L, Ratter JM, Hijmans A, Hooiveld GJ, Joosten LA, Rodenburg RJ, Fransen JA, Houtkooper RH, van CR, Netea MG, Stienstra R. 2016. Microbial stimulation of different Toll-like receptor signalling pathways induces diverse metabolic programmes in human monocytes. Nat Microbiol 2:16246. https://doi.org/10.1038/nmicrobiol.2016.246.
21. Fensterheim BA, Young JD, Luan L, Kleinbard RR, Stothers CL, Patil NK, McAtee-Pereira AG, Guo Y, Trenary I, Hernandez A, Fults JB, Williams DL, Sherwood ER, Bohannon JK. 2018. The TLR4 agonist monophosphoryl lipid A drives broad resistance toinfection via dnamic reprogramming of macrophage metabolism. J Immunol 200:3777–3789. https://doi.org/10.4049/jimmunol.1800085.
22. Lacey CA, Mitchell WJ, Brown CR, Skyberg JA. 2017. Temporal role for MyD88 in a model of *Brucella*-induced arthritis and musculoskeletal inflammation. Infect Immun 85:e00961-16. https://doi.org/10.1128/IAI.00961-16.
23. Corbel MJ. 1997. Brucellosis: an overview. Emerg Infect Dis 3:213–221. https://doi.org/10.3201/eid0302.970219.
24. Lacey CA, Chambers CA, Mitchell WJ, Skyberg JA. 2019. IFN-γ-dependent nitric oxide suppresses *Brucella*-induced arthritis by inhibition of inflammasome activation. J Leukoc Biol 106:27–34. https://doi.org/10.1002/JLB.4MIA1018-409R.
25. Skyberg JA, Lacey CA. 2017. Hematopoietic MyD88 and IL-18 are essential for IFN-gamma-dependent restriction of type A *Francisella tularensis* infection. J Leukoc Biol 102:1441–1450. https://doi.org/10.1189/jlb.4A0517-179R.
26. Copin R, De Baetselier P, Carlier Y, Letesson JJ, Muraille E. 2007. MyD88-dependent activation of B220-CD11b+LY-6C+ dendritic cells during *Brucella melitensis* infection. J Immunol 178:5182–5191. https://doi.org/10.4049/jimmunol.178.8.5182.
27. Xavier MN, Winter MG, Spees AM, den Hartigh AB, Nguyen K, Roux CM, Silva TM, Atluri VL, Kerrinnes T, Keestra AM, Monack DM, Luciw PA, Eigenheer RA, Baumler AJ, Santos RL, Tsolis RM. 2013. PPARγ-mediated increase in glucose availability sustains chronic *Brucella abortus* infection in alternatively activated macrophages. Cell Host Microbe 14:159–170. https://doi.org/10.1016/j.chom.2013.07.009.
28. Hong PC, Tsolis RM, Ficht TA. 2000. Identification of genes required for chronic persistence of *Brucella abortus* in mice. Infect Immun 68:4102–4107. https://doi.org/10.1128/IAI.68.7.4102-4107.2000.
29. Nair S, Huynh JP, Lampropoulou V, Loginicheva E, Esaulova E, Gounder AP, Boon ACM, Schwarzkopf EA, Bradstreet TR, Edelson BT, Artyomov MN, Stallings CL, Diamond MS. 2018. Irg1 expression in myeloid cells prevents immunopathology during *M. tuberculosis* infection. J Exp Med 215:1035–1045. https://doi.org/10.1084/jem.20180118.
30. Naujoks J, Tabeling C, Dill BD, Hoffmann C, Brown AS, Kunze M, Kempa S, Peter A, Mollenkopf HJ, Dorhoi A, Kershaw O, Gruber AD, Sander LE, Witzenrath M, Herold S, Nerlich A, Hocke AC, van D I, Suttorp N, Bedoui S, Hilbi H, Trost M, Opitz B. 2016. IFNs modify the proteome of *Legionella*-containing vacuoles and restrict infection via IRG1-derived itaconic acid. PLoS Pathog 12:e1005408. https://doi.org/10.1371/journal.ppat.1005408.
31. Michelucci A, Cordes T, Ghelfi J, Pailot A, Reiling N, Goldmann O, Binz T, Wegner A, Tallam A, Rausell A, Buttini M, Linster CL, Medina E, Balling R, Hiller K. 2013. Immune-responsive gene 1 protein links metabolism to immunity by catalyzing itaconic acid production. Proc Natl Acad Sci U S A 110:7820–7825. https://doi.org/10.1073/pnas.1218599110.
32. Jung M, Shim S, Im YB, Park WB, Yoo HS. 2018. Global gene-expression profiles of intracellular survival of the BruAb2_1031 gene mutated *Brucella abortus* in professional phagocytes, RAW 264.7 cells. BMC Microbiol 18:82. https://doi.org/10.1186/s12866-018-1223-7.
33. Hersch SJ, Navarre WW. 2020. The *Salmonella* LysR family regulator RipR activates the SPI-13-encoded itaconate degradation cluster. Infect Immun 88:e00303-20. https://doi.org/10.1128/IAI.00303-20.
34. Lampropoulou V, Sergushichev A, Bambouskova M, Nair S, Vincent EE, Loginicheva E, Cervantes-Barragan L, Ma X, Huang SC, Griss T, Weinheimer CJ, Khader S, Randolph GJ, Pearce EJ, Jones RG, Diwan A, Diamond MS, Artyomov MN. 2016. Itaconate links inhibition of succinate dehydrogenase with macrophage metabolic remodeling and regulation of inflammation. Cell Metab 24:158–166. https://doi.org/10.1016/j.cmet.2016.06.004.
35. Cordes T, Wallace M, Michelucci A, Divakaruni AS, Sapcariu SC, Sousa C, Koseki H, Cabrales P, Murphy AN, Hiller K, Metallo CM. 2016. Immunoresponsive gene 1 and itaconate inhibit succinate dehydrogenase to modulate intracellular succinate levels. J Biol Chem 291:14274–14284. https://doi.org/10.1074/jbc.M115.685792.
36. Lacey CA, Keleher LL, Mitchell WJ, Brown CR, Skyberg JA. 2016. CXCR2 mediates *Brucella*-induced arthritis in interferon gamma-deficient mice. J Infect Dis 214:151–160. https://doi.org/10.1093/infdis/jiw087.
37. Jessop F, Buntyn R, Schwarz B, Wehrly T, Scott D, Bosio CM. 2020. Interferon gamma reprograms host mitochondrial metabolism through inhibition of complex II to control intracellular bacterial replication. Infect Immun 88:e00744-19. https://doi.org/10.1128/IAI.00744-19.
38. Pham OH, O'Donnell H, Al-Shamkhani A, Kerrinnes T, Tsolis RM, McSorley SJ. 2017. T cell expression of IL-18R and DR3 is essential for non-cognate stimulation of Th1 cells and optimal clearance of intracellular bacteria. PLoS Pathog 13:e1006566. https://doi.org/10.1371/journal.ppat.1006566.
39. Archambaud C, Salcedo SP, Lelouard H, Devilard E, de BB, Van RN, Gorvel JP, Malissen B. 2010. Contrasting roles of macrophages and dendritic cells in controlling initial pulmonary *Brucella* infection. Eur J Immunol 40:3458–3471. https://doi.org/10.1002/eji.201040497.
40. Huang L, Nazarova EV, Tan S, Liu Y, Russell DG. 2018. Growth of *Mycobacterium tuberculosis in vivo* segregates with host macrophage metabolism and ontogeny. J Exp Med 215:1135–1152. https://doi.org/10.1084/jem.20172020.
41. Sasikaran J, Ziemski M, Zadora PK, Fleig A, Berg IA. 2014. Bacterial itaconate degradation promotes pathogenicity. Nat Chem Biol 10:371–377. https://doi.org/10.1038/nchembio.1482.
42. Skyberg JA, Thornburg T, Kochetkova I, Layton W, Callis G, Rollins MF, Riccardi C, Becker T, Golden S, Pascual DW. 2012. IFN-gamma-deficient mice develop IL-1-dependent cutaneous and musculoskeletal inflammation during experimental brucellosis. J Leukoc Biol 92:375–387. https://doi.org/10.1189/jlb.1211626.
43. Price JV, Russo D, Ji DX, Chavez RA, DiPeso L, Lee AY, Coers J, Vance RE. 2019. IRG1 and inducible nitric oxide synthase act redundantly with other interferon-γ-induced factors to restrict intracellular replication of *Legionella pneumophila*. mBio 10:e0269-19. https://doi.org/10.1128/mBio.02629-19.
44. Eoh H, Rhee KY. 2014. Methylcitrate cycle defines the bactericidal essentiality of isocitrate lyase for survival of *Mycobacterium tuberculosis* on fatty

acids. Proc Natl Acad Sci U S A 111:4976–4981. https://doi.org/10.1073/pnas.1400390111.
45. Abdou E, Jimenez de Bagues MP, Martinez-Abadia I, Ouahrani-Bettache S, Pantesco V, Occhialini A, Al DS, Kohler S, Jubier-Maurin V. 2017. RegA plays a key role in oxygen-dependent establishment of persistence and in isocitrate lyase activity, a critical determinant of *in vivo Brucella suis* pathogenicity. Front Cell Infect Microbiol 7:186. https://doi.org/10.3389/fcimb.2017.00186.
46. Zuniga-Ripa A, Barbier T, Conde-Alvarez R, Martinez-Gomez E, Palacios-Chaves L, Gil-Ramirez Y, Grillo MJ, Letesson JJ, Iriarte M, Moriyon I. 2014. *Brucella* abortus depends on pyruvate phosphate dikinase and malic enzyme but not on Fbp and GlpX fructose-1,6-bisphosphatases for full virulence in laboratory models. J Bacteriol 196:3045–3057. https://doi.org/10.1128/JB.01663-14.
47. Eisele NA, Ruby T, Jacobson A, Manzanillo PS, Cox JS, Lam L, Mukundan L, Chawla A, Monack DM. 2013. *Salmonella* require the fatty acid regulator PPARdelta for the establishment of a metabolic environment essential for long-term persistence. Cell Host Microbe 14:171–182. https://doi.org/10.1016/j.chom.2013.07.010.
48. Skyberg JA, Thornburg T, Rollins M, Huarte E, Jutila MA, Pascual DW. 2011. Murine and bovine gammadelta T cells enhance innate immunity against *Brucella abortus* infections. PLoS One 6:e21978. https://doi.org/10.1371/journal.pone.0021978.
49. Datsenko KA, Wanner BL. 2000. One-step inactivation of chromosomal genes in *Escherichia coli* K-12 using PCR products. Proc Natl Acad Sci U S A 97:6640–6645. https://doi.org/10.1073/pnas.120163297.
50. England JC, Perchuk BS, Laub MT, Gober JW. 2010. Global regulation of gene expression and cell differentiation in *Caulobacter crescentus* in response to nutrient availability. J Bacteriol 192:819–833. https://doi.org/10.1128/JB.01240-09.
51. Czyż DM, Willett JW, Crosson S. 2017. *Brucella abortus* induces a Warburg shift in host metabolism that Is linked to enhanced intracellular survival of the pathogen. J Bacteriol 199:e00227-17. https://doi.org/10.1128/JB.00227-17.
52. Lacey CA, Mitchell WJ, Dadelahi AS, Skyberg JA. 2018. Caspase-1 and caspase-11 mediate pyroptosis, inflammation, and control of *Brucella* joint infection. Infect Immun 86:e00361-18. https://doi.org/10.1128/IAI.00361-18.
53. Xia J, Psychogios N, Young N, Wishart DS. 2009. MetaboAnalyst: a web server for metabolomic data analysis and interpretation. Nucleic Acids Res 37:W652–W660. https://doi.org/10.1093/nar/gkp356.
54. Chambers CA, Lacey CA, Brown DC, Skyberg JA. 7 February 2021. Nitric oxide impairs IL-1 mediated protection against Escherichia coli K1-induced sepsis and meningitis in a neonatal murine model. Immunol Cell Biol https://doi.org/10.1111/imcb.12445.